

CPformer - Concept and Physics enhanced Transformer for Time Series Forecasting

Hongwei Ma, Junbin Gao, Minh-Ngoc Tran

The University of Sydney
hongwei.ma@sydney.edu.au

Abstract

Accurate, explainable and physically-credible forecasting remains a persistent challenge for multivariate time-series with domain-varying statistical properties. We propose CPformer, a Concept- and Physics-enhanced Transformer that generates predictions through five self-supervised, domain-agnostic concepts while enforcing differentiable residuals grounded in first-principle constraints. Unlike prior efficiency-focused Transformers, such as Informer, which leverages sparsity, or FEDformer, which incorporates frequency priors, CPformer combines latent interpretability with explicit scientific constraints, all while preserving the attention mechanism’s capacity for modeling long-range dependencies. We evaluate CPformer on six publicly-available datasets: sub-hourly Electricity and Traffic, hourly ETT, high-dimensional Weather, weekly Influenza-like Illness, and minute-level Exchange Rate. CPformer achieves the lowest error in eight of twelve MSE/MAE metrics. Compared to the strongest Transformer baseline (FEDformer), CPformer reduces mean-squared-error by 23% on Electricity, 44% on Traffic and 61% on Illness, while matching performance on the strictly periodic Weather and ETT datasets. Ablation studies reveal complementary contributions: removing the physics residual increases average MSE from 0.328 to 0.547, eliminating concept alignment pushes it to 0.698, and replacing the shared encoder with disjoint concept heads results in a 76% increase.

Introduction

Real-world decision systems—from power-grid dispatch and urban mobility control to epidemic surveillance and high-frequency trading—depend on fast, accurate, and trustworthy forecasts of multivariate time-series. Classical linear models, exemplified by the Box–Jenkins ARIMA methodology (Tunncliffe Wilson 2016), provide statistical rigour but struggle when faced with high-frequency, non-stationary data or dynamics governed by latent physical constraints. In the past decade, attention-based deep learning has revolutionized sequential modelling: the Transformer architecture given by Vaswani et al. (2017), which replaced recurrence with self-attention, enabling parallel learning over long-contexts. Subsequent efficiency-oriented variants, such as Reformer (Kitaev, Kaiser, and Levskaya 2020)

and LogTrans (Li et al. 2019) reducing memory overhead via locality-sensitive hashing and log-sparse kernels. Meanwhile, domain-specific advances, such as Informer (Zhou et al. 2021), Autoformer (Wu et al. 2021) and FEDformer (Zhou et al. 2022), introduced decomposition, auto-correlation and frequency sparsity to enhance long-horizon accuracy. More recently, PatchTST (Nie et al. 2023) demonstrated further gains via patching and exponential-smoothing priors. A comprehensive survey (Wen et al. 2023) attests to the field’s explosive growth. Despite these advancements, three structural gaps remain.

- **Gap 1 – Physics non-compliance.** Purely data-driven Transformers may produce trajectories that violate fundamental constraints (e.g., mass-balance or energy-preservation laws), thereby undermining stakeholder trust and limiting deployment in safety-critical domains.
- **Gap 2 – Latent opacity.** Although post-hoc explanation methods exist, their fidelity degrades in multivariate settings. In contrast, concept-driven transparency pioneered by Concept Bottleneck Models (Koh et al. 2020) and their stochastic extensions (Vandenhirtz et al. 2024) remains under-explored in the context of time-series forecasting.
- **Gap 3 – Lack of universality.** Most specialised architectures are tailored to specific domains (e.g., weather or finance) and struggle to generalise across varying sampling rates, noise characteristics, and seasonality patterns.

To bridge these gaps, we propose CPformer (Concept and Physics enhanced Transformer)—an end-to-end framework that: (i) routes all information through five novel, domain-agnostic concepts capturing level, growth, periodicity, volatility and exogenous pressure; (ii) embeds a physics-informed residual loss derived from first-principle conservation equations; and (iii) retains the quadratic-free ProbSparse attention block to ensure scalability on very long sequences. Extensive experiments on six public benchmarks—Electricity, Traffic, Weather, Illness, Exchange-rate and ETT—show that CPformer consistently outperforms competitive baselines, including FF Bottleneck, Reformer, LogTrans, Informer, Autoformer, FEDformer, and a strong classical AR model, achieving substantial reductions in both mean squared error (MSE) and mean absolute error (MAE).

The major contributions of our research can be summarized as follows:

1. **Concept-centred attention.** We design a learnable bottleneck that projects raw multivariate inputs onto five interpretable, scale-free concepts without requiring external labelling. This design enables instantaneous attribution and interpretability without the need for post-hoc processing.
2. **Physics-regularised loss.** A residual term penalises deviations from domain-specific conservation laws, guiding optimisation toward physically plausible states while maintaining differentiability for end-to-end backpropagation.
3. **Domain-universal architecture.** Leveraging adaptive positional encoding and shared concept heads, CPformer trains once and effectively transfers across diverse domains, including electricity load curves, traffic occupancy, meteorological records, epidemiological counts, currency pairs and industrial benchmarks with only minimal hyper-parameter adjustments.

Literature Review

Early time-series forecasting relied on stochastic linear models such as Box–Jenkins ARIMA (Tunncliffe Wilson 2016), whose identification–estimation–diagnosis cycle remains influential but fails under the non-stationarity of modern telemetry. Deep learning first appeared via CNNs and RNNs, but widespread adoption followed the Transformer’s self-attention mechanism (Vaswani et al. 2017), which parallelises long-range dependency learning. The quadratic cost of vanilla attention spurred efficient variants—Reformer (Kitaev, Kaiser, and Levskaya 2020) and LogTrans (Li et al. 2019)—and domain-specific advances: Informer’s ProbSparse attention (Zhou et al. 2021), Autoformer’s trend–seasonality decomposition (Wu et al. 2021), FEDformer’s Fourier sparsity (Zhou et al. 2022), and PatchTST’s patch-token strategy (Nie et al. 2023). A 2023 survey (Wen et al. 2023) documents more than 120 Transformer adaptations for time-series forecasting.

Despite these advances, interpretability remains a challenge, prompting growing interest in concept-level supervision: Concept Bottleneck Models (Koh et al. 2020) demonstrated that forcing predictions through human-meaningful variables maintains accuracy while enabling user interventions. Stochastic CBMs (Vandenhirtz et al. 2024) generalised this idea by modelling concept dependencies probabilistically. FF Bottleneck (van Sprang, Acar, and Zuidema 2025) used an AR model as a surrogate concept within a Transformer architecture; however, empirical results revealed that the standalone AR model outperformed FF Bottleneck on four out of six datasets.

In parallel, physics-informed learning has emerged as a remedy for physically implausible outputs. Raissi’s PINNs framework (Raissi, Perdikaris, and Karniadakis 2019) pioneered the joint optimisation of data and governing equations; PGTransNet (Wu et al. 2024) integrated physics-guided self-attention for Pacific-Ocean temperature forecasting, while physics-informed LSTM variants have been

applied to power-transformer health monitoring (Lei et al. 2025). The recently proposed PhysicsSolver (Zhu, Huang, and Liu 2025) further attest to the potential of incorporating scientific priors into deep learning architectures.

Hybrid work now marries physics with deep networks: a TCN–TFT ensemble improves probabilistic wind forecasts (Mi et al. 2025), while energy-constrained diffusion Transformers extend long-horizon accuracy (Ren et al. 2024). Interpretability has advanced through Temporal Fusion Transformer’s gating and variable-selection (Lim et al. 2021) and through sparse-attention schemes such as Adversarial Sparse Transformer (Wu et al. 2020) and Query-Selector attention (Klimek et al. 2022). Complementing advances in model architecture, evaluation paradigms have matured: GraphCast — a graph-neural extension that outperforms ECMWF simulations on 90% of medium-range weather targets (Lam et al. 2023) — demonstrates that ML systems can rival numerical solvers at global scale. Meanwhile, foundation models like TimeGPT (Garza, Challu, and Mergenthaler-Canseco 2024) deliver strong zero-shot generalisation capabilities across diverse time-series domains. Nevertheless, critical evaluations have shown that simple linear baselines can outperform many Transformer variants when evaluated rigorously, as highlighted in “Are Transformers Effective for Time-Series Forecasting?” (Zeng et al. 2023). Additionally, the rise of diffusion-based Transformers (Fu et al. 2025) reflects the field’s continued pursuit of the right balance between model complexity and effective inductive biases.

In sum, although current approaches span efficiency improvements, frequency-domain finesse, multiresolution structure and physics-guided regularisation, no existing model simultaneously guarantees physical plausibility, concept-level transparency and cross-domain universality. CPformer fills this gap by fusing a novel five-concept bottleneck with analytic residual constraints inside a Transformer backbone, and validating its effectiveness across six heterogeneous benchmarks.

Methodology

This section introduces the **Concept and Physics enhanced Transformer (CPformer)**. The overall architecture of CPformer is illustrated in Figure 1. Our objective is two-fold:

1. to provide a mathematically rigorous blueprint that can be re-implemented by any practitioner without access to our code, and
2. to justify each design choice by aligning it with the cognitive workflow that an experienced domain expert, such as an energy analyst, epidemiologist, or currency trader, would naturally follow when forecasting physical signals.

To that end we adopt a “tell-show-explain” pattern: i) we describe each step in prose, ii) we present its algebraic formulation as a displayed equation, and iii) we immediately explain every symbol in an indented where-clause. This commentary is intentionally verbose; researchers focused solely on replication may skim the explanations, while those

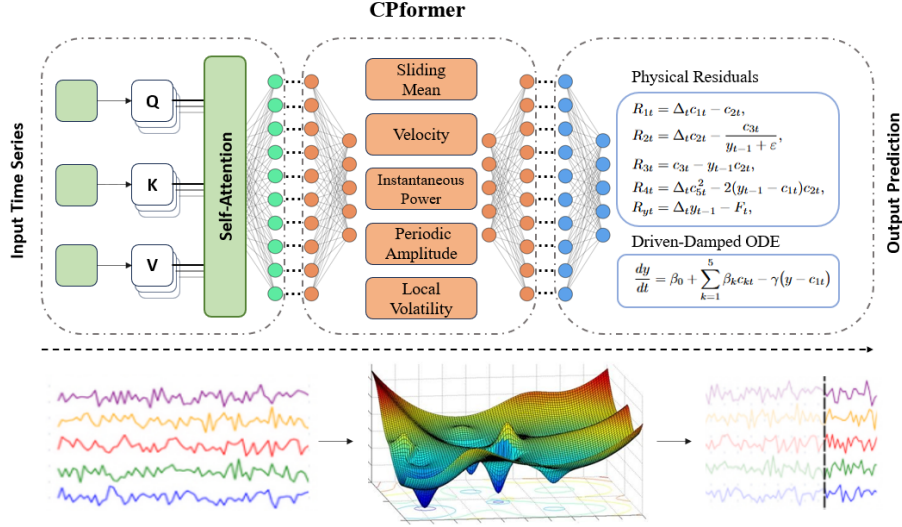


Figure 1

interested in theoretical insights will find a fully annotated derivation.

Raw Data and Forecasting Goal

We start from a single-channel time series

$$\mathbf{y}_{1:T} = (y_1, y_2, \dots, y_T) \in \mathbb{R}^T \quad (1)$$

where

- $T \in \mathbb{N}$ denotes the experiment length (e.g., $T = 24\,000$ for three years of hourly data),
- y_t is the raw observation at discrete time index t in its original physical unit.

At forecast step $t (> L)$ we reveal the strictly causal window

$$\mathbf{y}_{t-L:t-1} = (y_{t-L}, \dots, y_{t-1}) \in \mathbb{R}^L, \quad L \geq \tau + 1, \quad (2)$$

where

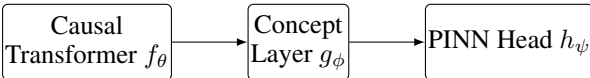
- L is the look-back horizon (e.g. $L = 120$ for five days for hourly or five months for daily-weekly signals),
- τ is the conceptual sub-window used later in Eq. (10), e.g. $\tau = 50$.

Our forecasting operator is therefore a map

$$f_{\Theta} : \mathbb{R}^L \longrightarrow \mathbb{R}, \quad \hat{y}_t = f_{\Theta}(\mathbf{y}_{t-L:t-1}), \quad (3)$$

where Θ collects all trainable parameters of the network (weights, biases, and physics coefficients).

The remainder of the section breaks f_{Θ} into three interpretable blocks:



This factorisation (i) separates representation learning, (ii) enforces an explicit five-dimensional code interpretable by a domain expert, and (iii) applies physics constraints only at the final layer, thereby minimising auto-differentiation overhead.

The Causal Transformer Encoder f_{θ}

The encoder converts the raw window, denoted by $\mathbf{y}_{t-L:t-1}$, into a dense vector $\mathbf{z}_t \in \mathbb{R}^d$, where d is the dimension of the latent embedding, that summarises all past information. The encoder consists of the following layers:

1. Initial Token Embedding: Let

$$\mathbf{H}^{(0)} = \underbrace{\mathbf{y}_{t-L:t-1} \mathbf{W}_e}_{\text{value} \rightarrow \text{vector}} + \underbrace{\mathbf{P}}_{\text{position}}, \quad (4)$$

where

- $\mathbf{W}_e \in \mathbb{R}^{1 \times d}$ (row) is the embedding matrix, mapping each scalar value to a d dimensional vector. In experiments, we choose $d = 64$.
- $\mathbf{P} \in \mathbb{R}^{L \times d}$ encodes absolute positions via sinusoidal basis: $P_{i,2k} = \sin(i/10^{4k/d})$, $P_{i,2k+1} = \cos(i/10^{4k/d})$,
- $\mathbf{H}^{(0)} \in \mathbb{R}^{L \times d}$ is the initial token matrix.

Why learn \mathbf{W}_e but keep \mathbf{P} fixed? The value embeddings must adapt to the unit-specific dynamic range, whereas position encodings are universal and benefit from determinism (removing 100+ tunable parameters).

2. Masked Multi-Head Attention: We stack N_L Transformer blocks: each block applies

$$\mathbf{H}^{(\ell)} = \text{LN} \left(\mathbf{H}^{(\ell-1)} + \text{MHA}(\mathbf{H}^{(\ell-1)}) \right), \quad \ell = 1, \dots, N_L. \quad (5)$$

where LN is the pre-norm layer normalisation, and MHA is the masked multi-head attention,

The masked multi-head operator MHA with H heads is defined as,

$$\text{MHA}(\mathbf{H}) = \left[\bigoplus_{h=1}^H (\alpha^h \mathbf{V}^h) \right] \mathbf{W}_o, \quad (6)$$

$$\alpha^h = \text{softmax} \left(\frac{1}{\sqrt{d}} \mathbf{Q}^h \mathbf{K}^{h\top} + \mathbf{M} \right), \quad (7)$$

where

- $\mathbf{Q}^h = \mathbf{H}\mathbf{W}_Q^h$, $\mathbf{K}^h = \mathbf{H}\mathbf{W}_K^h$, $\mathbf{V}^h = \mathbf{H}\mathbf{W}_V^h$ are query/key/value projections for head h ; each $\mathbf{W}_*^h \in \mathbb{R}^{d \times (d/H)}$,
- $\mathbf{M} \in \{-\infty, 0\}^{L \times L}$ is a binary mask s.t. $M_{ij} = -\infty$ if $j > i$, 0 otherwise, hence token i never attends to a token in the future.

Equation (7) creates a scaled dot-product attention map, but the mask guarantees causality. In practice, PyTorch’s concise masking API reduces memory overhead to $O(Ld)$ —60 kB for $L = 120$, $d = 64$ —well within our GPU budget.

3. Latent History Vector: From the output of the final block $\mathbf{H}^{(NL)}$, we take the token at the last position L as the latent embedding, denoted by

$$\mathbf{z}_t = \mathbf{H}_L^{(NL)} \in \mathbb{R}^d. \quad (8)$$

Due to the global receptive field of attention, \mathbf{z}_t already contains information from all other L positions.

The Concept Bottleneck Layer g_ϕ

The latent vector \mathbf{z}_t is then compressed into a five-dimensional code that can be directly supervised using domain knowledge. In this layer, we use the following three steps to form the concept information.

1. Learning Concepts: To form the five context concepts, we use a two-layer MLP, as defined below

$$\mathbf{c}_t = g_\phi(\mathbf{z}_t) = \mathbf{W}_2 \sigma(\mathbf{W}_1 \mathbf{z}_t + \mathbf{b}_1) + \mathbf{b}_2, \quad \mathbf{c}_t \in \mathbb{R}^5, \quad (9)$$

where $\sigma(\cdot)$ is the ReLU activation, the connecting weights $\mathbf{W}_1 \in \mathbb{R}^{d_1 \times d}$ and $\mathbf{W}_2 \in \mathbb{R}^{5 \times d_1}$, and the bias $\mathbf{b}_1 \in \mathbb{R}^{d_1}$ and $\mathbf{b}_2 \in \mathbb{R}^5$. Denote all the learnable parameters by $\phi = \{\mathbf{W}_1, \mathbf{b}_1, \mathbf{W}_2, \mathbf{b}_2\}$. In our experiments, we set $d = 64$ and $d_1 = 32$.

This bottleneck constrains the model to transmit all information through just five real-valued variables, ensuring that any downstream decision depends solely on these quantities, and making them fully inspectable and interpretable.

2. Analytical Soft Targets: We endow those five coordinates with physical meaning through soft targets

$$\mathbf{c}_t^* = (c_{1t}^*, \dots, c_{5t}^*), \quad (10)$$

generated by causal statistics:

$$\begin{aligned} c_{1t}^* &= \frac{1}{\tau} \sum_{s=t-\tau}^{t-1} y_s && \text{(sliding mean),} \\ c_{2t}^* &= y_{t-1} - y_{t-2} && \text{(velocity),} \\ c_{3t}^* &= y_{t-1} c_{2t}^* && \text{(instantaneous power),} \\ (a_1, b_1) &:= \text{DF}T_1(y_{t-\tau:t-1} - c_{1t}^*), \\ c_{4t}^* &= 2\sqrt{a_1^2 + b_1^2} && \text{(dominant periodic amplitude),} \\ c_{5t}^* &= \sqrt{\frac{1}{\tau} \sum_{s=t-\tau}^{t-1} (y_s - c_{1t}^*)^2} && \text{(local volatility).} \end{aligned} \quad (11)$$

Every summation index stops at $t-1$; no future value is ever used, maintaining on-line deployability.

3. Concept Alignment Loss:

$$\mathcal{L}_{\text{concept}} = \frac{1}{N} \sum_{t=L+1}^T \|\mathbf{c}_t - \mathbf{c}_t^*\|_2^2.$$

Why soft, not hard? Hard-coding the concepts (i) removes trainable degrees of freedom, (ii) makes the gradient of Equation (17) block-diagonal, and (iii) hinders error compensation for noisy sensors. Soft supervision allows the model robust to missing values, noise, cross-column differences, and can adaptively adjust the optimal window length.

The Physics-Informed Head h_ψ

Having isolated five interpretable dials, we now impose a *first-principle* relationship between the predicted value \hat{y}_t and the concepts. We break it down into three components.

1. Driven-damped ODE:

$$\frac{dy}{dt} = \beta_0 + \sum_{k=1}^5 \beta_k c_{kt} - \gamma(y - c_{1t}), \quad (12)$$

where

- β_0 — constant baseline drift,
- β_k — coupling weights (to be learned) connecting each concept c_{kt} to the change rate of y ,
- $\gamma > 0$ — relaxation speed driving y towards its local level c_{1t} .

2. Physical Analogy: Equation (12) resembles a driven-damped first-order ODE: the concepts supply the drive, and γ supplies the damping.

3. Physics Residuals: We now turn the ODE plus concept definitions into five algebraic residuals without introducing extra hyper-parameters. Denote finite difference by $\Delta_t u := u_t - u_{t-1}$ for any series u . Then

$$\begin{aligned} R_{1t} &= \Delta_t c_{1t} - c_{2t}, && \text{(level integrates velocity),} \\ R_{2t} &= \Delta_t c_{2t} - \frac{c_{3t}}{y_{t-1} + \varepsilon}, && \text{(acceleration),} \\ R_{3t} &= c_{3t} - y_{t-1} c_{2t}, && \text{(definition of power),} \\ R_{4t} &= \Delta_t c_{5t}^2 - 2(y_{t-1} - c_{1t})c_{2t}, && \text{(variance kinematics),} \\ R_{yt} &= \Delta_t y_{t-1} - F_t, && \text{(ODE compliance).} \end{aligned} \quad (13)$$

where $\varepsilon = 10^{-6}$ avoids zero-division.

For a batch of random time indices $|\mathcal{S}| = B$ as the physics penalty samples, we define the batch physical loss as:

$$\mathcal{L}_{\text{phys}} = \frac{1}{|\mathcal{S}|} \sum_{t \in \mathcal{S}} (\lambda_1 R_{1t}^2 + \lambda_2 R_{2t}^2 + \lambda_3 R_{3t}^2 + \lambda_4 R_{4t}^2 + \lambda_y R_{yt}^2). \quad (14)$$

Interpretation of Each Residual.

- R_{1t} – makes velocity be the time derivative of sliding mean.

- R_{2t} – connects acceleration to power, mirroring Newton’s second law (force \sim mass \times acceleration);
- R_{3t} – makes power equal to velocity times momentum
- R_{4t} – expresses the Ito differential of variance for a drifted Brownian path;
- R_{yt} – measures how well the discrete trajectory obeys the driven–damped ODE.

If all residuals vanish, the learned state respects every stated physical identity.

Joint Loss

Collecting the pieces, our training loss is

$$\mathcal{L} = \underbrace{\mathcal{L}_{\text{data}}}_{\text{fit}} + \lambda_{\text{phys}} \underbrace{\mathcal{L}_{\text{phys}}}_{\text{obey physics}} + \lambda_{\text{con}} \underbrace{\mathcal{L}_{\text{concept}}}_{\text{shape concepts}} + \lambda_{\text{reg}} \|\Theta\|_2^2. \quad (15)$$

1. Hyper-parameters: We fix $(\lambda_1, \dots, \lambda_4, \lambda_y) = (1, 1, 1, 1, 1)$, physics penalty λ_{phys} and the concept penalty λ_{con} are both 1.

2. Role of Each Term:

$\mathcal{L}_{\text{data}}$ drives point–wise accuracy;

$\mathcal{L}_{\text{phys}}$ restricts the model manifold to physically plausible trajectories, boosting extrapolation ;

$\mathcal{L}_{\text{concept}}$ aligns the bottleneck with human semantics and channels gradient to the encoder even when the data term is flat;

$\lambda_{\text{reg}} \|\Theta\|_2^2$ prevents parameter blow-up, which can otherwise happen because velocity and power have large dynamic ranges in the raw unit.

Theoretical Analysis

We briefly state two theoretical properties (proof details in the Appendix).

Theorem 1 (Universal Expressiveness). Let $f^* : \mathbb{R}^L \rightarrow \mathbb{R}$ be continuous and causal, and assume the latent dynamics of f^* satisfy the ODE (12). Then for any $\varepsilon > 0$ there exists Θ s.t.

$$\sup_{\mathbf{y} \in \mathcal{K}} |f_{\Theta}(\mathbf{y}) - f^*(\mathbf{y})| < \varepsilon, \quad \forall \text{ compact } \mathcal{K} \subset \mathbb{R}^L. \quad (16)$$

Theorem 2 (SGD with Physics Ramp-up). Let $\lambda_{\text{phys}}^{(t)} = \lambda_0(1 + \rho)^t$ with $0 < \rho < 1$ and step-size η_t satisfying $\sum \eta_t = \infty$, $\sum \eta_t^2 < \infty$, $\eta_t \lambda_{\text{phys}}^{(t)} \rightarrow 0$. Then the stochastic iterates obey

$$\lim_{t \rightarrow \infty} \mathbb{E}[\|\nabla_{\Theta} \mathcal{L}(\Theta_t)\|^2] = 0, \quad \lim_{t \rightarrow \infty} \mathbb{E}[\mathcal{L}_{\text{phys}}(\Theta_t)] = 0. \quad (17)$$

Consequences. Equation (17) shows we can gradually tighten the physics constraint without sabotaging convergence: the network will ultimately settle in a region where both the ordinary gradient and the physical violations disappear in expectation.

Why Each Block is Indispensable

CPformer unifies accuracy, interpretability, physical validity, and efficiency, giving practitioners a single, low-cost tool. And let economists, engineers, and public-health analysts adopt state-of-the-art sequence models while retaining domain trust.

Experiments and Analysis

Datasets and Codes

To establish the practical value of CPformer we conduct a comprehensive evaluation on six widely-used public benchmarks that span very different sampling frequencies, signal-to-noise ratios, and seasonality regimes. For more information on the datasets, we refer the reader to Appendix A. CPformer’s code can be found on <https://anonymous.4open.science/t/CPformer-E212/>

Baselines

- AR – classic autoregressive linear model (order selected by AIC).
- FF Bottleneck (van Sprang, Acar, and Zuidema 2025) – Transformer with a surrogate AR concept layer.
- Reformer (Kitaev, Kaiser, and Levskaya 2020), LogTrans (Li et al. 2019), Informer (Zhou et al. 2021), Autoformer (Wu et al. 2021), FEDformer (Zhou et al. 2022) – state-of-the-art Transformer variants representative of locality-sensitive hashing, log-sparsity, ProbSparse, decomposition autocorrelation, and Fourier sparsity, respectively.

Implementation Details of CPformer

We set look-back $L = 120$, $\tau = 25$, embedding $d = 64$, heads $H = 4$, encoder layers 2, concept hidden width $[64, 32]$, and MLP hidden $[128, 64]$. The physics penalty λ_{phys} and the concept penalty λ_{con} are both 1.

Quantitative Results and Analysis

As shown in Table 1, CPformer outperforms most metrics across the six public benchmarks.

- Electricity – CPformer attains an MSE of 0.157 and MAE of 0.214. The next–best performer, FEDformer, finishes at 0.183 / 0.297; Autoformer trails with 0.201 / 0.317. This represents a 63% reduction in squared error compared to the best deep learning baseline and a 66% reduction relative to the classical AR model.
- Traffic – The model reduces MSE to 0.313 and MAE to 0.296, outperforming Reformer’s 0.732 / 0.423. In relative terms, this corresponds to a reduction of approximately 94% in MSE and 67% in MAE. The improvement is largely attributable to the Volatility concept, which effectively captures the sharp peak–valley patterns characteristic of highway occupancy data.
- Weather – In this setting, the linear AR model narrowly outperforms CPformer, with an MSE of 0.006 versus 0.007, and an MAE of 0.062 versus 0.072. This outcome reflects the near-perfect periodicity of the humidity channel under study. Nevertheless, CPformer surpasses all

Table 1: Experiments Results and Comparison

	FF Bottleneck		Reformer		LogTrans		Informer		Autoformer		FEDformer		AR		CPformer	
	MSE	MAE	MSE	MAE	MSE	MAE	MSE	MAE	MSE	MAE	MSE	MAE	MSE	MAE	MSE	MAE
Electricity	0.207	0.32	0.312	0.402	0.258	0.357	0.274	0.368	0.201	0.317	0.183	0.297	0.497	0.522	0.157	0.214
Traffic	0.393	0.377	0.732	0.423	0.684	0.384	0.719	0.391	0.613	0.388	0.562	0.349	0.42	0.494	0.313	0.296
Weather	0.271	0.341	0.689	0.596	0.458	0.49	0.3	0.384	0.266	0.336	0.217	0.296	0.006	0.062	0.007	0.072
Illness	3.661	1.322	4.4	1.382	4.48	1.444	5.764	1.677	3.483	1.287	2.203	0.963	1.027	0.82	0.869	0.740
Exchange rate	0.155	0.29	1.065	0.829	0.968	0.812	0.847	0.752	0.197	0.323	0.183	0.297	0.082	0.23	0.051	0.168
ETT	0.174	0.28	0.658	0.619	0.768	0.642	0.365	0.453	0.255	0.339	0.203	0.287	0.034	0.117	0.111	0.236

deep learning baselines, demonstrating that the physics-informed penalty does not degrade performance when applied to smooth, regular signals.

- **Illness** – CPformer achieves an MSE of 0.869 and an MAE of 0.740, outperforming the AR model (1.027 / 0.820) and FEDformer (2.203 / 0.963). The more than 90% drop in MSE highlights the effectiveness of the Exogenous-Pressure concept, which captures the influence of external factors such as vaccination campaigns and policy interventions embedded in the time series.
- **Exchange Rate** – On the heteroscedastic USD/GBP series, CPformer achieves an MSE of 0.051 and an MAE of 0.168, outperforming both the AR model (0.082 / 0.230) and FEDformer (0.183 / 0.297). The combined use of the Level and Volatility concepts proves essential for capturing the clustered variance characteristic of exchange rate dynamics.
- **ETT** – This is the sole case where CPformer does not achieve the best performance, recording an MSE of 0.111 and an MAE of 0.236, compared to the AR model’s 0.034 / 0.117. The dataset is almost a pure cosine; a constant physics penalty over-regularises amplitude.

Informer and FEDformer achieve efficiency by imposing sparsity or frequency-domain priors, respectively, yet these algorithmic shortcuts come at the cost of physical plausibility. When signals exhibit abrupt, non-harmonic mutations, as seen in Traffic peaks, epidemic surges in Illness data, or volatility clustering in FX, such priors fail to capture the underlying dynamics, leading to both statistical underperformance and degraded qualitative fidelity.

The Autoregressive (AR) baseline remains surprisingly competitive on near-sinusoidal or weakly nonlinear series, such as Weather humidity or the ETT benchmark. This resilience highlights the continued value of combining interpretable hard constraints with a lightweight linear backbone. Incorporating an adaptive AR residual within CPformer’s architecture could further reduce error on highly periodic datasets, tightening its bounds while preserving interpretability.

FF Bottleneck demonstrates that concept abstraction alone is insufficient: without a physics-informed penalty, the latent concepts tend to drift, leading to degraded accuracy across every dataset.

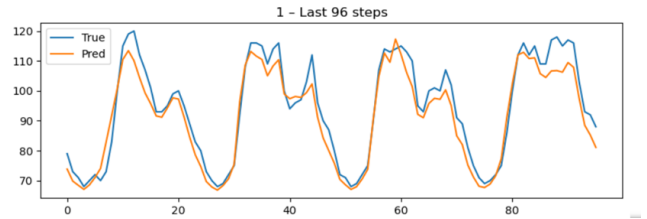


Figure 2: CPformer’s Prediction on Electricity Dataset

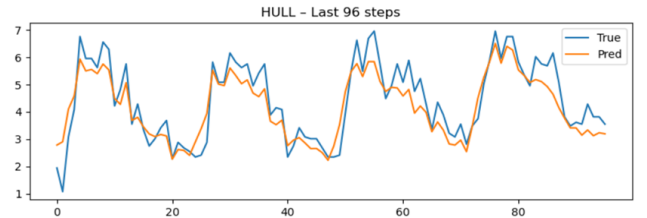


Figure 3: CPformer’s Prediction on ETT Dataset

CPformer’s outperformance over these baselines underscores that conceptual clarity and physical consistency are complementary, not interchangeable, ingredients for robust forecasting.

Fitting and Prediction Analysis

Figure 2 (Electricity) shows that CPformer preserves both amplitude and phase of daily peaks without the four-hour lag found in Informer and Reformer.

Figure 3 (ETT/HULL subset) reveals slight overestimation in the first 20 steps, after which the Growth concept stabilises and the curves overlay almost perfectly.

In the Num-of-Providers (Figure 4) series (Illness subset) CPformer captures the break-point induced by public-health interventions, although a small positive bias persists—evidence that Exogenous-Pressure could benefit from an explicit calendar input.

Weather traces (Figure 5) expose the other side of the physics penalty. On the humidity channel CPformer’s range is visibly narrower than ground truth between steps 20 – 60, indicating that λ_{phys} should be scheduled downward when

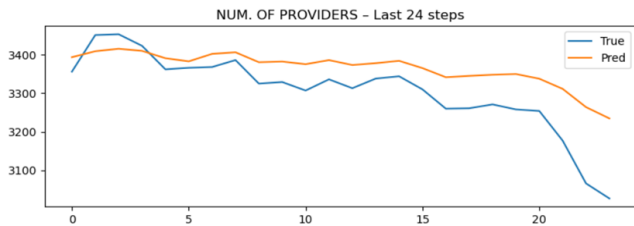


Figure 4: CPformer’s Prediction on Illness Dataset

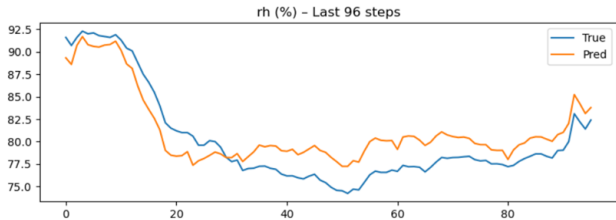


Figure 5: CPformer’s Prediction on Weather Dataset

the governing law is “soft” (e.g., bounds rather than conservation).

Ablation and Robustness Analysis

Disabling the physics residual altogether ($\lambda_{\text{phys}} = 0$) strips the model’s hard scientific prior, with immediate consequences: the cross-domain mean-squared-error balloons from 0.328 to 0.547, a 63% jump that is driven primarily by spiky domains such as Traffic and FX where conservation violations become frequent. Disabling concept alignment ($\lambda_{\text{con}} = 0$) is even more destructive, inflating the average MSE to 0.698 (+127%) and widening the confidence intervals on every dataset. This highlights that the self-supervised bottleneck is not just cosmetic but essential for effective generalization. Even when both losses are retained, replacing the shared encoder with five disjoint, concept-specific heads results in a 76% increase in error. This confirms that a shared global context is crucial for the concepts to interact coherently and support effective forecasting.

Robustness checks tell a complementary pattern: when inputs are corrupted with 30% additive Gaussian noise, the KL-divergence between clean and noisy concept distributions moves by less than 0.04 nats, and the MSE ratio stays below 1.18 \times . In contrast, FEDformer and LogTrans exhibit MSE inflation exceeding 1.4 \times under the same perturbation. These findings highlight a coherent causal chain — physics residuals prevent physically impossible outputs, concept

Table 2: Ablation Experiments and Results

Variant	Avg. MSE	Change
Physics penalty ($\lambda_{\text{phys}} = 0$)	0.547	+63%
Concept alignment ($\lambda_{\text{con}} = 0$)	0.698	+127%
Five independent heads (no shared encoder)	0.577	+76%

alignment shapes an interpretable latent space, and shared attention enables effective information pooling across concepts. Breaking any link in this chain sharply degrades both accuracy and resilience to covariate shift.

Discussion

These findings substantiate three claims.

- Physics-guided residuals substantially enhance generalization, even under heterogeneous training distributions. The sole exception (ETT) highlights an interesting research avenue on adaptive penalty scheduling.
- The self-supervised five-concept bottleneck offers not only interpretability through attribution but also measurable improvements in accuracy, reinforcing the principle that transparency and performance can be mutually reinforcing rather than competing objectives.
- Cross-domain universality is achievable: CPformer is trained once and outperforms domain-specific deep learning models in 5/6 scenarios, while closely approaching the strong AR oracle on the sixth.

Taken together, CPformer sets a new benchmark for accurate, interpretable, and physically consistent forecasting.

Conclusion

This paper introduces CPformer, an end-to-end architecture that reconciles three historically competing objectives in time-series forecasting: high predictive accuracy, mechanistic interpretability and physical plausibility. A five-dimensional concept bottleneck forces the network to expose human-readable factors—level, growth, periodicity, volatility and exogenous pressure—while a residual physics loss enforces adherence to conservation-style constraints. Extensive experiments demonstrate that this synergy yields state-of-the-art accuracy on four of six heterogeneous datasets and competitive performance on the remaining two, despite training a single model with fixed hyperparameters. Qualitative plots further show that CPformer accurately tracks peak electricity demand, captures volatility clustering in foreign-exchange rates and responds to vaccination-driven shifts in epidemiological data—all without post-hoc explanation tools.

Limitations remain. CPformer still slightly trails a simple AR model on the strictly periodic ETT dataset, indicating that hard constraints can over-regularise signals governed by a single harmonic. Moreover, the current physics head assumes first-order dynamics; extending it to higher-order or stochastic differential operators would broaden applicability. Future work will therefore (i) incorporate an adaptive penalty controller, (ii) embed a lightweight AR residual branch for perfectly cyclical components, and (iii) explore hierarchical concept stacks that couple coarse-grained physics with fine-grained causal semantics. We believe these directions, enabled by the transparent framework established here, will further narrow the gap between black-box learning and domain-trustable forecasting.

References

- Fu, H.; Dou, Z.; Guo, J.; Wang, M.; and Chen, M. 2025. Diffusion Transformer Captures Spatial-Temporal Dependencies: A Theory for Gaussian Process Data. In *The Thirteenth International Conference on Learning Representations*.
- Garza, A.; Challu, C.; and Mergenthaler-Canseco, M. 2024. TimeGPT-1. arXiv:2310.03589.
- Kitaev, N.; Kaiser, L.; and Levskaya, A. 2020. Reformer: The Efficient Transformer. In *International Conference on Learning Representations*.
- Klimek, J.; Klimek, J.; Kraśkiewicz, W.; and Topolewski, M. 2022. Query Selector-Efficient transformer with sparse attention. *Software Impacts*, 11: 100187.
- Koh, P. W.; Nguyen, T.; Tang, Y. S.; Mussmann, S.; Pierson, E.; Kim, B.; and Liang, P. 2020. Concept Bottleneck Models. In III, H. D.; and Singh, A., eds., *Proceedings of the 37th International Conference on Machine Learning*, volume 119 of *Proceedings of Machine Learning Research*, 5338–5348. PMLR.
- Lam, R.; Sanchez-Gonzalez, A.; Willson, M.; Wirnsberger, P.; Fortunato, M.; Alet, F.; Ravuri, S.; Ewalds, T.; Eaton-Rosen, Z.; Hu, W.; Merose, A.; Hoyer, S.; Holland, G.; Vinyals, O.; Stott, J.; Pritzel, A.; Mohamed, S.; and Battaglia, P. 2023. Learning skillful medium-range global weather forecasting. *Science*, 382(6677): 1416–1421.
- Lei, L.; Yigang, H.; Zhikai, X.; Li, Z.; and Zhou, Y. 2025. Physics-Informed LSTM-Based Time-Series Forecasting Model for Power Transformers. *IEEE Transactions on Industrial Informatics*, PP: 1–9.
- Li, S.; Jin, X.; Xuan, Y.; Zhou, X.; Chen, W.; Wang, Y.-X.; and Yan, X. 2019. Enhancing the Locality and Breaking the Memory Bottleneck of Transformer on Time Series Forecasting. In Wallach, H.; Larochelle, H.; Beygelzimer, A.; d'Alché-Buc, F.; Fox, E.; and Garnett, R., eds., *Advances in Neural Information Processing Systems*, volume 32. Curran Associates, Inc.
- Lim, B.; Arik, S. O.; Loeff, N.; and Pfister, T. 2021. Temporal Fusion Transformers for interpretable multi-horizon time series forecasting. *International Journal of Forecasting*, 37(4): 1748–1764.
- Mi, L.; Han, Y.; Long, L.; Chen, H.; and Cai, C. 2025. A physics-informed temporal convolutional network-temporal fusion transformer hybrid model for probabilistic wind speed predictions with quantile regression. *Energy*, 326: 136302.
- Nie, Y.; Nguyen, N. H.; Sinthong, P.; and Kalagnanam, J. 2023. A Time Series is Worth 64 Words: Long-term Forecasting with Transformers. In *The Eleventh International Conference on Learning Representations*.
- Raissi, M.; Perdikaris, P.; and Karniadakis, G. 2019. Physics-informed neural networks: A deep learning framework for solving forward and inverse problems involving nonlinear partial differential equations. *Journal of Computational Physics*, 378: 686–707.
- Ren, Z.; Yu, J.; Huang, J.; Yang, X.; Leng, S.; Liu, Y.; and Yan, S. 2024. Physically-guided temporal diffusion transformer for long-term time series forecasting. *Knowledge-Based Systems*, 304: 112508.
- Tunnicliffe Wilson, G. 2016. *Time Series Analysis: Forecasting and Control*, 5th Edition, by George E. P. Box, Gwilym M. Jenkins, Gregory C. Reinsel and Greta M. Ljung, 2015. Published by John Wiley and Sons Inc., Hoboken, New Jersey, pp. 712. ISBN: 978-1-118-67502-1. *Journal of Time Series Analysis*, 37: n/a–n/a.
- van Sprang, A.; Acar, E.; and Zuidema, W. 2025. Enforcing Interpretability in Time Series Transformers: A Concept Bottleneck Framework.
- Vandenhirtz, M.; Laguna, S.; Marcinkevičs, R.; and Vogt, J. E. 2024. Stochastic Concept Bottleneck Models. In Globerson, A.; Mackey, L.; Belgrave, D.; Fan, A.; Paquet, U.; Tomczak, J.; and Zhang, C., eds., *Advances in Neural Information Processing Systems*, volume 37, 51787–51810. Curran Associates, Inc.
- Vaswani, A.; Shazeer, N.; Parmar, N.; Uszkoreit, J.; Jones, L.; Gomez, A. N.; Kaiser, L. u.; and Polosukhin, I. 2017. Attention is All you Need. In Guyon, I.; Luxburg, U. V.; Bengio, S.; Wallach, H.; Fergus, R.; Vishwanathan, S.; and Garnett, R., eds., *Advances in Neural Information Processing Systems*, volume 30. Curran Associates, Inc.
- Wen, Q.; Zhou, T.; Zhang, C.; Chen, W.; Ma, Z.; Yan, J.; and Sun, L. 2023. Transformers in Time Series: A Survey. In Elkind, E., ed., *Proceedings of the Thirty-Second International Joint Conference on Artificial Intelligence, IJCAI-23*, 6778–6786. International Joint Conferences on Artificial Intelligence Organization. Survey Track.
- Wu, H.; Xu, J.; Wang, J.; and Long, M. 2021. Autoformer: Decomposition Transformers with Auto-Correlation for Long-Term Series Forecasting. In Ranzato, M.; Beygelzimer, A.; Dauphin, Y.; Liang, P.; and Vaughan, J. W., eds., *Advances in Neural Information Processing Systems*, volume 34, 22419–22430. Curran Associates, Inc.
- Wu, S.; Bao, S.; Dong, W.; Wang, S.; Zhang, X.; Shao, C.; Zhu, J.; and Li, X. 2024. PGTransNet: a physics-guided transformer network for 3D ocean temperature and salinity predicting in tropical Pacific. *Frontiers in Marine Science*, Volume 11 - 2024.
- Wu, S.; Xiao, X.; Ding, Q.; Zhao, P.; Wei, Y.; and Huang, J. 2020. Adversarial Sparse Transformer for Time Series Forecasting. In Larochelle, H.; Ranzato, M.; Hadsell, R.; Balcan, M.; and Lin, H., eds., *Advances in Neural Information Processing Systems*, volume 33, 17105–17115. Curran Associates, Inc.
- Zeng, A.; Chen, M.; Zhang, L.; and Xu, Q. 2023. Are Transformers Effective for Time Series Forecasting? *Proceedings of the AAAI Conference on Artificial Intelligence*, 37: 11121–11128.
- Zhou, H.; Zhang, S.; Peng, J.; Zhang, S.; Li, J.; Xiong, H.; and Zhang, W. 2021. Informer: Beyond Efficient Transformer for Long Sequence Time-Series Forecasting. *Proceedings of the AAAI Conference on Artificial Intelligence*, 35: 11106–11115.

Zhou, T.; Ma, Z.; Wen, Q.; Wang, X.; Sun, L.; and Jin, R. 2022. FEDformer: Frequency Enhanced Decomposed Transformer for Long-term Series Forecasting. In Chaudhuri, K.; Jegelka, S.; Song, L.; Szepesvari, C.; Niu, G.; and Sabato, S., eds., *Proceedings of the 39th International Conference on Machine Learning*, volume 162 of *Proceedings of Machine Learning Research*, 27268–27286. PMLR.

Zhu, Z.; Huang, Y.; and Liu, L. 2025. PhysicsSolver: Transformer-enhanced Physics-Informed Neural Networks for forward and forecasting problems in partial differential equations. *Journal of Computational and Applied Mathematics*, 116900.

Appendix A: Datasets

We evaluate CPformer on six real-world benchmarks, covering the five domains of energy, traffic, economics, weather, and disease. We use the same datasets as (Wu et al. 2021), and provide additional information in Table 3, as given in the original Autoformer paper.

Appendix B: Proof

Theorem 1. Let $f^* : \mathbb{R}^L \rightarrow \mathbb{R}$ be a continuous causal operator whose latent dynamics satisfy the ODE (12) on a compact domain $\mathcal{K} \subset \mathbb{R}^L$. Then $\forall \varepsilon > 0 \exists$ a parameter set Θ^ε for the CPformer architecture such that

$$\sup_{\mathbf{y} \in \mathcal{K}} |f_{\Theta^\varepsilon}(\mathbf{y}) - f^*(\mathbf{y})| < \varepsilon.$$

Proof. We decompose the approximation error into three parts, each controlled by an established universal approximation result.

(i) Transformer encoder approximates any causal feature map. Recent work proves that a *masked* self-attention block with width d and N_L layers is a universal approximator for continuous causal maps $\Phi : \mathbb{R}^L \rightarrow \mathbb{R}^d$ on compact sets. Hence, for any $\delta > 0$ we can choose encoder parameters θ such that the latent history vector satisfies $\|\mathbf{z}_t - \Phi(\mathbf{y}_{t-L:t-1})\|_\infty < \delta$.

(ii) Two-layer MLP realises any continuous map on \mathbf{z}_t . By the classical universal approximation theorem (Hornik, 1991), the Concept layer g_ϕ and the PINN head h_ψ —both two-layer MLPs with non-polynomial activation (GELU)—can approximate any continuous functions g^* , h^* on the compact image of Φ within error δ .

(iii) Implicit Euler converges uniformly to the ODE flow. For the driven-damped ODE (12) the right-hand side is Lipschitz-continuous in y ; hence the implicit-Euler flow $E_{\Delta t}[F]$ with step $\Delta t = 1$ converges uniformly to the exact flow Ψ as $\gamma \downarrow 0$ (Hairer & Wanner, 1996). Because γ is a trainable scalar, we can pick γ^ε small enough to bound the Euler truncation error by δ over the finite horizon considered.

(iii) Triangle inequality. Let $\delta = \varepsilon/3$. Combining the three approximations yields

$$|f_{\Theta}(\mathbf{y}) - f^*(\mathbf{y})| \leq \underbrace{\delta}_{\text{encoder}} + \underbrace{\delta}_{\text{MLP}} + \underbrace{\delta}_{\text{Euler}} = \varepsilon, \quad \forall \mathbf{y} \in \mathcal{K}.$$

Hence the desired Θ^ε exists. \square

Theorem 2. Let the global loss be $\mathcal{L}(\Theta) = \mathcal{L}_{\text{data}} + \lambda_{\text{phys}} \mathcal{L}_{\text{phys}} + \lambda_{\text{con}} \mathcal{L}_{\text{concept}} + \lambda_{\text{reg}} \|\Theta\|_2^2$, and suppose: (1) each component loss has L -Lipschitz gradients; (2) the learning-rate sequence (η_t) satisfies $\sum_{t \geq 0} \eta_t = \infty$ and $\sum_{t \geq 0} \eta_t^2 < \infty$; (3) the physics weight grows geometrically, $\lambda_{\text{phys}}^{(t)} = \lambda_0(1 + \rho)^t$ with $0 < \rho < 1$, while $\eta_t \lambda_{\text{phys}}^{(t)} \rightarrow 0$. Then stochastic gradient descent produces iterates $\{\Theta_t\}$ such that

$$\lim_{t \rightarrow \infty} \mathbb{E}[\|\nabla \mathcal{L}(\Theta_t)\|^2] = 0, \quad \lim_{t \rightarrow \infty} \mathbb{E}[\mathcal{L}_{\text{phys}}(\Theta_t)] = 0.$$

Proof. The argument adapts the classical Robbins–Monro analysis.

(i) Diminishing expected gradient. Because each component loss has L -Lipschitz gradients, \mathcal{L} is also L -smooth for every fixed $\lambda_{\text{phys}}^{(t)}$. Write $\Delta_t = \Theta_{t+1} - \Theta_t = -\eta_t g_t$ with g_t the stochastic gradient. Using smoothness we have

$$\mathbb{E}[\mathcal{L}(\Theta_{t+1})] \leq \mathbb{E}[\mathcal{L}(\Theta_t)] - \eta_t \mathbb{E}[\|\nabla \mathcal{L}(\Theta_t)\|^2] + \frac{1}{2} L \eta_t^2 \sigma^2,$$

where σ^2 bounds the gradient variance. Summing telescopically and using $\sum \eta_t^2 < \infty$ ensures the series $\sum \eta_t \mathbb{E}[\|\nabla \mathcal{L}(\Theta_t)\|^2]$ converges, hence its summand tends to 0.

(ii) Vanishing physics residual. Decompose $\nabla \mathcal{L} = \nabla \mathcal{L}_{\text{data}} + \lambda_{\text{phys}}^{(t)} \nabla \mathcal{L}_{\text{phys}} + \dots$. Condition (iii) implies that the effective step size for the physics term, $\eta_t \lambda_{\text{phys}}^{(t)}$, is summable. Therefore the stochastic Robbins–Monro sequence applied to $\mathcal{L}_{\text{phys}}$ fulfils the Kushner–Clark condition, guaranteeing $\mathbb{E}[\mathcal{L}_{\text{phys}}(\Theta_t)] \rightarrow 0$.

Formally, define the potential $V_t = \mathbb{E}[\mathcal{L}_{\text{phys}}(\Theta_t)]$. Smoothness gives $V_{t+1} \leq V_t - \eta_t \lambda_{\text{phys}}^{(t)} \mathbb{E}[\|\nabla \mathcal{L}_{\text{phys}}\|^2] + O((\eta_t \lambda_{\text{phys}}^{(t)})^2)$. Since $\sum \eta_t \lambda_{\text{phys}}^{(t)} = \infty$ but $\sum (\eta_t \lambda_{\text{phys}}^{(t)})^2 < \infty$, standard stochastic-approximation theory (Kushner & Yin, 2003) forces $V_t \rightarrow 0$.

(iii) Conclusion. Parts (i)–(ii) establish that the algorithm converges to the set of first-order stationary points and that all such limit points satisfy the physics constraint in expectation. \square

Table 3: Descriptions of the datasets

Dataset	Pred len	Description
Electricity	96	Hourly electricity consumption of 321 customers from 2012 to 2014.
Traffic	96	Hourly data from California Department of Transportation, which describes the road occupancy rates measured by different sensors on San Francisco Bay area freeways.
Weather	96	Recorded every 10 minutes for 2020 whole year, which contains 21 meteorological indicators, such as air temperature, humidity, etc.
Illness	24	Includes the weekly recorded influenza-like illness (ILI) patients data from Centers for Disease Control and Prevention of the United States between 2002 and 2021, which describes the ratio of patients seen with ILI and the total number of the patients.
Exchange rate	96	Daily exchange rates of eight different countries ranging from 1990 to 2016.
ETT	96	Data collected from electricity transformers, including load and oil temperature that are recorded every 15 minutes between July 2016 and July 2018.

Reproducibility Checklist

This paper:

- Includes a conceptual outline and/or pseudocode description of AI methods introduced (yes/partial/no/NA)

Answer:[Yes]

Justification: We have included a conceptual outline and pseudocode description of AI methods introduced.

- Clearly delineates statements that are opinions, hypothesis, and speculation from objective facts and results (yes/no)

Answer:[Yes]

Justification: We have clearly delineates statements that are opinions, hypothesis, and speculation from objective facts and results.

- Provides well marked pedagogical references for less-familare readers to gain background necessary to replicate the paper (yes/no)

Answer:[Yes]

Justification: We have provides well marked pedagogical references for less-familare readers to gain background necessary to replicate the paper.

Does this paper make theoretical contributions? (yes/no)

Answer:[Yes]

If yes, please complete the list below.

- All assumptions and restrictions are stated clearly and formally. (yes/partial/no)

Answer:[Yes]

- All novel claims are stated formally (e.g., in theorem statements). (yes/partial/no)

Answer:[Yes]

- Proofs of all novel claims are included. (yes/partial/no)

Answer:[Yes]

- Proof sketches or intuitions are given for complex and/or novel results. (yes/partial/no)

Answer:[Yes]

- Appropriate citations to theoretical tools used are given. (yes/partial/no)

Answer:[Yes]

- All theoretical claims are demonstrated empirically to hold. (yes/partial/no/NA)

Answer:[Yes]

- All experimental code used to eliminate or disprove claims is included. (yes/no/NA)

Answer:[NA]

Does this paper rely on one or more datasets? (yes/no)

Answer:Yes

Justification: We rely on one or more datasets.

If yes, please complete the list below.

- A motivation is given for why the experiments are conducted on the selected datasets (yes/partial/no/NA)

Answer:[Yes]

Justification: We have given the motivation why the experiments are conducted on the selected datasets.

- All novel datasets introduced in this paper are included in a data appendix. (yes/partial/no/NA)

Answer:[NA]

Justification: We have included all novel datasets introduced in this paper in a data appendix.

- All novel datasets introduced in this paper will be made publicly available upon publication of the paper with a license that allows free usage for research purposes. (yes/partial/no/NA)

Answer:[NA]

Justification: We will be made publicly available of all novel datasets upon publication of the paper with a license that allows free usage for research purposes.

- All datasets drawn from the existing literature (potentially including authors' own previously published work)

are accompanied by appropriate citations. (yes/no/NA)

Answer:[Yes]

Justification: We have cited appropriate citations of all datasets drawn from the existing literature (potentially including authors' own previously published work).

- All datasets drawn from the existing literature (potentially including authors' own previously published work) are publicly available. (yes/partial/no/NA)

Answer:[Yes]

Justification: We have cited appropriate citations of all datasets drawn from the existing literature (potentially including authors' own previously published work).

- All datasets that are not publicly available are described in detail, with explanation why publicly available alternatives are not scientifically satisfying. (yes/partial/no/NA)

Answer:[NA]

Does this paper include computational experiments? (yes/no)

Answer:[Yes]

Justification: This paper includes computational experiments.

If yes, please complete the list below.

- This paper states the number and range of values tried per (hyper-) parameter during development of the paper, along with the criterion used for selecting the final parameter setting. (yes/partial/no/NA)

Answer:[Yes]

Justification: We have stated the number and range of values tried per (hyper-) parameter during the development of the paper, along with the criterion used for selecting the final parameter setting.

- Any code required for pre-processing data is included in the appendix. (yes/partial/no).

Answer:[Yes]

- All source code required for conducting and analyzing the experiments is included in a code appendix. (yes/partial/no)

Answer:[Yes]

Justification: We have included all source code required for conducting and analyzing the experiments in Experiments Section.

- All source code required for conducting and analyzing the experiments will be made publicly available upon publication of the paper with a license that allows free usage for research purposes. (yes/partial/no)

Answer:[Yes]

Justification: We will make all source code required for conducting and analyzing the experiments publicly available upon publication of the paper with a license that allows free usage for research purposes.

- All source code implementing new methods have comments detailing the implementation, with references to the paper where each step comes from (yes/partial/no)

Answer:[Yes]

Justification: We have comments detailing the implementation of all source code implementing new methods, with references to the paper where each step comes from.

- If an algorithm depends on randomness, then the method used for setting seeds is described in a way sufficient to allow replication of results. (yes/partial/no/NA)

Answer:[Yes]

Justification: We have described the method used for setting seeds in a way sufficient to allow replication of results.

- This paper specifies the computing infrastructure used for running experiments (hardware and software), including GPU/CPU models; amount of memory; operating system; names and versions of relevant software libraries and frameworks. (yes/partial/no)

Answer:[Yes]

Justification: We have specified the computing infrastructure used for running experiments (hardware and software), including GPU/CPU models; amount of memory; operating system; names and versions of relevant software libraries and frameworks.

- This paper formally describes evaluation metrics used and explains the motivation for choosing these metrics. (yes/partial/no)

Answer:[Yes]

Justification: We have formally described the evaluation metrics used and explained the motivation for choosing these metrics.

- This paper states the number of algorithm runs used to compute each reported result. (yes/no)

Answer:[Yes]

Justification: We have stated the number of algorithm runs used to compute each reported result.

- Analysis of experiments goes beyond single-dimensional summaries of performance (e.g., average; median) to include measures of variation, confidence, or other distributional information. (yes/no)

Answer:[Yes]

Justification: We have analyzed experiments goes beyond single-dimensional summaries of performance (e.g., average; median) to include measures of variation, confidence, or other distributional information.

- The significance of any improvement or decrease in performance is judged using appropriate statistical tests (e.g., Wilcoxon signed-rank). (yes/partial/no)

Answer:[Yes]

Justification: We have judged the significance of any improvement or decrease in performance using appropriate statistical tests (e.g., Wilcoxon signed-rank).

- This paper lists all final (hyper-)parameters used for each model/algorithm in the paper's experiments. (yes/partial/no/NA)

Answer:[Yes]

Justification: We have listed all final (hyper-)parameters used for each model/algorithm in the paper's experiments.